Comparison of the effects of two municipal sewage treatment process discharge on receiving rivers in plateau habitats

Jun Wang[a], Jiaao Ji[a], Xianpai Peng[a], Yongchen Zong[a,*], Chunhui Fu[a], Dongyan Zhang[a,b]

[a]_Water Conservancy Project and Civil Engineering College, Tibet Agricultural and Animal Husbandry University, Linzhi 860000, China, emails: zyc_2001@sohu.com (Y. Zong), wang_jun1998@163.com (J. Wang), 243274931@qq.com (J. Ji), 290491614@qq.com (X. Peng), 1354599589@qq.com (C. Fu), 593968038@qq.com (D. Zhang)_
[b]_Huazhong University of Science and Technology, State Key Laboratory of Coal Combustion, Wuhan 430074, China_

ABSTRACT

Microbiological and metabolomic analyses based on Illumina MiSeq high-throughput sequencing technology were carried out on the receiving rivers in upland habitats to compare the impacts of effluent discharges from two urban wastewater treatment processes on the receiving rivers. The results showed that microbial diversity increased in the lower reaches of the receiving rivers, but the overall microbial diversity of the rivers in the plateau habitat was lower than that in the plains. _Proteobacteria_ (47.4%–57.04%) and _Sphingorhabdus_ (25%–32.19%) were both the most abundant phylum and genus in the upper and lower reaches of the two feeder rivers. The effects of anaerobic-anoxic-aerobic (AAO) vs. artificial wetland (CW) effluent discharge on microbial community abundance showed either an increase or a decrease, but analysis of _Luteolibacter_, an indicator bacterium of good water quality, found that abundance increased by 4.01% downstream of the AAO receiving river. Analysis of the downstream trend of dominant genera abundance suggests that the AAO receiving river has a stronger self-purification of pollutants and recovery of dominant genera. In terms of carbon, nitrogen, and phosphorus metabolic pathways and gene expression, AAO and CW treatment processes showed different significant effects on the receiving rivers and even had completely opposite effects on some functional modules. In addition, the AAO receiving river showed better recoverability in terms of carbon and phosphorus metabolic pathways. This study reveals the microbiological and carbon, nitrogen, and phosphorus metabolomic responses of the receiving rivers to sewage discharge in plateau habitats and provides a new practical idea and perspective for the selection of sewage treatment processes and sewage discharge in plateau towns.

Keywords: Receiving rivers; Plateau habitats; Microbial communities; Metabolic pathways

1. Introduction

Tibet is located in the southwest of China, at the third pole of the earth, with special environmental factors such as high altitude, low temperature, and low pressure [1]. The surface water area in Tibet is vast and mainly originates from snow and ice melt. According to the survey, rivers in the plateau environment have a special environment that differs greatly from those in the plains. It features low water temperatures, high water velocity, high sand content, riverbeds covered with gravel, and few aquatic plants. The rivers in this region have a low microbial content and probably have less resistance to the increased concentration of pollutants in the rivers. Therefore, the microbial community structure and metabolic response mechanisms of the receiving rivers were analyzed based on the plateau habitat and the town wastewater treatment plants (WWTPs).

* Corresponding author.

The impact of WWTPs on receiving rivers depends mainly on the type of treatment process and the volume of effluent discharged [2]. The anaerobic-anoxic-aerobic (AAO) process is known to be the most utilized wastewater treatment process for WWTPs in towns and cities in Tibet [3,4], followed by artificial wetlands (CW). The AAO process is a traditional mainstream process with advantages such as simplicity of operation. Artificial wetland is an artificially constructed biological treatment process that simulates natural environmental conditions and has features such as low operating costs. Therefore, the AAO process and artificial wetlands are widely used in the Tibetan Plateau region for sewage treatment. Given that the population density in the Tibetan plateau region is much lower than that in the plains, it has a smaller WWTP scale in its towns and cities, and the proportion of sewage discharge to the flow of the receiving rivers is quite small. Thus, the region does not have a large-scale increase in the high concentration of pollutants brought about by sewage discharge, which can alleviate the problem of less resistant river microorganisms in the plateau habitat.

WWTPs sewage discharge leads to excess nutrients in rivers [5], affecting nutrient uptake efficiency [6]. Microbial community structure in rivers is also significantly affected by effluent discharge [7], including several functional bacterial communities: denitrifying bacterial communities [8], ammonia-oxidizing assemblages [9], among others. Related studies have shown that WWTP significantly affects denitrification rates downstream of receiving rivers [10,11]. In addition, nitrification dominates nitrogen cycling below WWTP outfalls [12]. However, there is no literature available on the functional modules of carbon, nitrogen, and phosphorus metabolism and gene expression in response to effluent discharge in receiving rivers. Therefore, this study is the first to analyze the functional modules of carbon, nitrogen, and phosphorus metabolism and gene expression in receiving rivers in an upland habitat.

In this context, this study compares the effects of two mainstream municipal sewage treatment processes on receiving rivers in a plateau environment. This includes water quality indicators, microbial diversity, and community structure before and after the outfall of the receiving rivers, as well as some functional module pathways and genes in carbon, nitrogen, and phosphorus metabolic pathways that are significantly affected by the effluent discharge. The microbial and metabolic response mechanisms were then analyzed using Illumina MiSeq high-throughput sequencing technology to provide an objective assessment of the impact of effluent discharge on rivers in plateau habitats.

2. Materials and methods

2.1. Description of sampling information

The fact is that the Tibetan region is sparsely populated, and the towns are far apart from each other. The two WWTPs (AAO and CW) are more than 160 km apart, but their receiving rivers are the same (Fig. 1). The receiving river contains a high sand content, with the bottom of the riverbed covered with gravel and little aquatic vegetation. In addition, both WWTPs use UV disinfection for tailwater treatment of sewage discharge.

Due to the special river environment in Tibet, the bottom of the river is covered with sand and gravel and does not contain mud. Because the river flows very fast and constantly scours the sand and gravel at the bottom of the river, it is difficult for sediments to exist at the bottom of the river and for the sediments to be sampled. Therefore, only river water samples were collected. In this study, water quality and microbiological samples were taken from the outfalls and upstream and downstream (both 100 m from the outfalls) of the receiving rivers in the two towns, with a total of six sampling points (AAO_SY, AAO_HR, AAO_XY, CW_SY, CW_HR, and CW_XY). There were no other tributaries between the upstream and downstream sampling points and the outfall. In addition, additional sampling of incoming and outgoing water quality and microbial sampling of the reaction tanks at the two WWTPs were conducted. Basic information on the WWTP and receiving rivers is shown in Tables 1 and 2.

2.2. Water quality and microbiological sampling

The water samples for water quality indicators were first placed in 500 mL collection bottles. Three parallel water samples were collected at each sampling point for subsequent averaging of the specific indicator values detected. 5 mL of sulfuric acid, pH < 2, was then added to each collection bottle. The collection bottles were stored at 0°C–5°C and tested within 3 d.

Water samples for microbiological sample filtration were placed in a 10 L collection bucket. Before microbiological sampling, the collection bucket is rinsed three times with river water from the sampling site to avoid the interference of microorganisms by other residues in the bucket. The microbial water samples were filtered immediately in the laboratory on the same day using a mixed fiber filter membrane with a pore size of 0.22 μm and a diameter of 100 mm. The microorganisms extracted in a short time were stored in a –80°C environment.

2.3. Determination and analytical methods

2.3.1. Conventional indicators

Chemical oxygen demand (COD) concentration was determined by the potassium dichromate method; ammonia

Table 1
WWTP project overview

Overview	AAO	CW
Average daily sewage treatment capacity (m^3)	900	1,800–1,900
Running time (y)	2	5
Altitude (m)	3,060	2,865
UV (mW/cm^2)	5.2	4.51
Effluent concentration		
NH$_3$–N (mg/L)	4.09	15.873
TP (mg/L)	0.247	0.7
TN (mg/L)	11.66	17.28
COD (mg/L)	40.735	40.012

Table 2
Receiving rivers parameter testing

| Parameter detection	AAO_SY	AAO_HR	AAO_XY	CW_SY	CW_HR	CW_XY
Temperature (°C)	8.8	10	8.8	7.1	7.6	7.3
Dissolved oxygen (mg/L)	10.88	10.94	11.04	12.3	11.3	10.82
Flow rate (m/s)	4.62	4.12	3.56	0.05	0.08	0.07
pH	8.63	8.7	8.8	8.57	8.47	8.06
Annual mean daily flow (m³)	9,720,000			2,980,800		
Flow on the sampled days (m³)	6,480,000			2,764,800		
Contribution of the effluent wastewater on the flow of the receiving water body (%)	0.014			0.067		
NH_3–N (mg/L)	0.532	2.034	0.481	0.445	2.867	0.438
TP (mg/L)	0.024	0.0783	0.036	0.027	0.1105	0.0165
TN (mg/L)	1.08	3.282	0.966	1.069	3.503	1.63
COD (mg/L)	15.019	28.0195	15.5425	8.145	26.343	20.2625
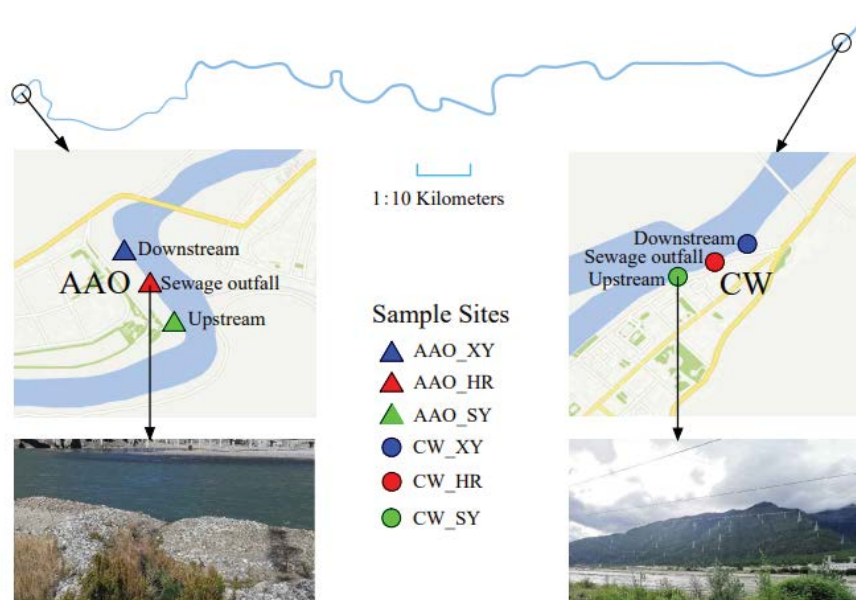
Fig. 1. Relative position of the two WWTPs and receiving rivers in AAO and CW. (AAO_SY, AAO_HR, and AAO_XY denote the upstream, the confluence of the effluent discharge with the river, and the downstream, respectively, of the AAO WWTP receiving river; CW_SY, CW_HR, and CW_XY denote the upstream, the confluence of the effluent discharge with the river, and the downstream, respectively, of the CW WWTP receiving river).

nitrogen (NH_3–N) concentration was determined by Nessler reagent spectrophotometry; total nitrogen (TN) concentration was determined by potassium persulfate UV spectrophotometry; total phosphorus (TP) concentration was determined by spectrophotometer; and DO and pH were determined by the HACH Multi-function Tester (HQ40d Field Case Cat No. 58258-00).

2.3.2. DNA extraction and 16S rRNA gene sequencing

To understand the functional properties of microorganisms and genes, 8 samples obtained in this pilot study (in a –80°C environment) were entrusted to Majorbio Biotechnology Co., Ltd., Shanghai, China, for sequencing (htpp://www.majorbio.com). The sequencing experiments first required the extraction of sample DNA using the Fast DNA Spin Kit (Fast DNA Spin Kit for Soil, MP, USA) [13], followed by detection using 1% agarose gel electrophoresis. Then a PCR instrument (ABI GeneAmp® Model 9700) was used to perform PCR amplification at the variable region (V3-V4) of the 16S rRNA gene using primers 338F (5′-ACTCCTACGGGAGGCAGCAG-3′) and 806R (5′-GGACTACHVGGGTWTCTAAT-3′). Three replicates of PCR amplification products from the same sample were mixed and detected by 2% agarose gel electrophoresis. The PCR products were quantified by QuantiFluor™-ST Blue Fluorescence Quantification System (Promega) with reference to the preliminary quantification results of

electrophoresis and then mixed in the appropriate proportion according to the sequencing volume required for each sample. The official Illumina splice sequence was added to the outer end of the target region by PCR, and the PCR product was recovered by cutting the gel using the AxyPrepDNA Gel Recovery Kit (AXYGEN), followed by elution with Tris-HCl buffer and detection by 2% agarose electrophoresis. After denaturation in NaOH, a single-stranded DNA fragment was obtained, and its fragment end was immobilized on the chip with complementary primer bases to synthesize the target DNA fragment to be tested, which forms the "bridge" after denaturation and annealing. DNA polymerase and dNTP were added, and the surface of the reaction plate was scanned with a laser to read the nucleotide species polymerized on the template sequence. Finally, the "fluorescent moiety" and "termination moiety" were chemically cleaved to restore the 3′ end adhesion and continue the polymerization of the second nucleotide, and the cycle was repeated, counting the sequences of the template DNA fragments obtained in each round, and then Illumina MiSeq sequencing was finished.

2.4. Data processing methods

The degree of abundance of species and functional modules affected by effluent discharge in this study was expressed through $\log_2$ fold change to facilitate comparison between species or functional modules with large differences in abundance. Analysis of variance (ANOVA) was carried out to disperse the $\log_2$ fold change values to compare whether the species and metabolic pathways in the two receiving rivers were better able to recover after being affected by the effluent discharge.

Based on information from the Kyoto Encyclopedia of Genes and Genomes database (KEGG, Kyoto Encyclopedia of Genes and Genomes, http://www.genome.jp/kegg/), this study used PICRUSt2 (a software package for functional prediction of 16S amplicon sequencing results) to obtain Information on the abundance of genes and functional modules in carbon, nitrogen, and phosphorus metabolic pathways.

Distance-based redundancy analysis (db-RDA) was used to relate microbial community structure to water quality indicator parameters by (1) calculating the Bray-Curtis distance matrix; (2) PCoA analysis; (3) creating a matrix of dummy variables; (4) using RDA to analyze the relationship between the principal coordinates (microbial data) and the dummy variables (model data); and (5) performing a db-RDA analysis. The correlation heatmap analysis was carried out with the aid of R (version 3.3.1) (pheatmap package) by calculating Spearman rank correlation coefficients between environmental factors and species and visualizing the obtained matrix of values in heatmap plots.

3. Results and discussion

3.1. Changes in water quality indicators of the receiving rivers

The effluent from both WWTPs (AAO and CW) is discharged into the same river, but the two outfalls are more than 160 km apart. It is considered that water quality indicators in the upstream and downstream of the CW WWTP's receiving river are not influenced by the AAO WWTP. This study provides a specific analysis of the trends in the mean concentrations of pollutants (ammonia nitrogen (NH_3–N), total phosphorus (TP), total nitrogen (TN), and COD) upstream, downstream, and at the confluence of the two receiving river sections (Table 2). The average NH_3–N concentrations in the AAO and CW receiving rivers followed the same trend, with significant increases at the outfall confluence (1.502 and 2.422 mg/L in the AAO and CW, respectively). Also, the concentrations decreased in the downstream compared with the upstream, and the changes were smaller (0.042 and 0.007 mg/L for AAO and CW, respectively), indicating that the receiving rivers are more resistant to changes in NH_3–N concentrations and have a certain self-purification capacity for NH_3–N.

Compared to upstream, mean TP concentrations increased by 0.012 mg/L downstream of the AAO receiving river and decreased by 0.0105 mg/L downstream of the CW. In addition, mean TP concentrations increased more at CW than at AAO at the confluence, indicating that the CW receiving river was more resistant to changes in TP concentrations compared to AAO. This is similar to the variation in NH_3–N concentrations, probably owing to the different water velocities in the two receiving rivers, with the CW receiving river having slower water velocities and more time for river microorganisms to degrade NH_3–N and TP. The average TN and COD concentrations decreased by 0.114 mg/L and increased by 0.5235 mg/L downstream of the AAO receiving river and increased by 0.561 and 12.1175 mg/L downstream of the CW receiving river, respectively. The trend of TN concentration in the AAO receiving river section was similar to that of CW. However, the trends in COD concentrations differed more, with a greater increase downstream of CW, probably due to the difficulty of river microorganisms in resisting CW discharges with high COD concentrations over short distances.

3.2. Effects of effluent on the diversity and species abundance of riverine microbial communities

The Alpha diversity in this study was quantified through species richness Chao, diversity Shannon, and evenness Shannoneven (Fig. 2). The coverage index ranged from 0.984 to 0.989, indicating that each sample was sampled to a standard that adequately reflects the true picture of the overall microbial community structure (Table S1). The increased species diversity downstream of both the AAO and CW receiving rivers compared to upstream may be largely attributed to the WWTP effluent discharge. The CW WWTP had a greater impact on species diversity downstream of the receiving river, increasing species richness downstream by 222 taxa compared to 65 taxa downstream of the AAO. The Shannon index showed an increase in microbial diversity at the confluence of the AAO receiving river and a decrease in diversity at the CW receiving river, which could be directly attributed to the opposing trends of impacts caused by tailwater discharge from the two different wastewater treatment processes, and a higher
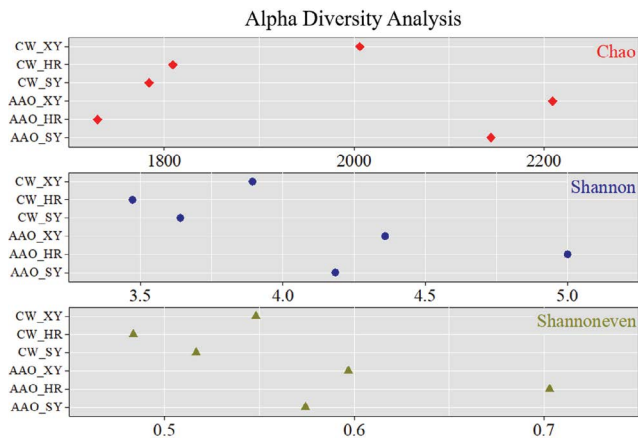
Fig. 2. Alpha diversity index analysis (richness index: Chao, diversity index: Shannon, evenness index: Shannoneven).

Fig. 3. Stacked histogram of the 10 most abundant dominant phyla in relative abundance.

microbial diversity in the entire AAO receiving river than in the CW. However, the index of river microbial diversity in the plateau environment was significantly lower than that in some plains rivers [14–16], indicating that the specific environmental factors in the plateau suppress microbial diversity [17,18]. Shannoneven index trends were consistent with Shannon.

At the phylum level, the most abundant phyla in the AAO WWTP included *Actinobacteriota* (43.75%), *Proteobacteria* (23.07%), *Patescibacteria* (10.55%), *Bacteroidota* (9.28%), *Chloroflexi* (6.72%), etc., and the most abundant phyla in the CW WWTP included *Bacteroidota* (27%), *Firmicutes* (19.64%), *Proteobacteria* (10.54%), *Actinobacteriota* (9.24%), and *Caldisericota* (7.01%) (Fig. S1). The abundance of dominant phyla varies widely due to different wastewater treatment processes.

In both receiving rivers, the top 10 phyla in relative abundance dominated the overall community structure (98.12% ~ 99.38%) (Fig. 3). *Proteobacteria* was the most abundant phylum, with significantly lower abundance ($p < 0.05$) at the outfalls (AAO_HR and CW_HR), mainly influenced by effluent discharge. There was no significant difference ($p > 0.05$) between the upstream and downstream reaches of the CW outfall, with better recoverability. *Actinobacteriota* increased significantly ($p < 0.05$) at the outfall, with a 51.78% increase at CW_HR, mainly influenced by the significance of the effluent discharge. However, *Actinobacteriota* (9.24%) was not the most abundant genus in the CW WWTP (Fig. S1), probably due to the favorable growth environment in the river (e.g., higher dissolved oxygen [19]), coupled with some nutrients provided by the wastewater discharge, which contributed to the rapid growth of this *Actinobacteriota*. *Bacteroidota* and *Verrucomicrobiota* were the third and fourth most abundant phyla, respectively, with opposite trends in the two effluent-bearing reaches of the AAO and CW. *Bacteroidota* decreased significantly (from 22.68% to 0.27%) at CW_HR ($p < 0.05$), and *Verrucomicrobiota* decreased significantly (from 8.09% to 0.46%) at AAO_HR. In addition, *Acidobacteriota* was virtually unaffected by effluent discharge throughout the AAO nadir, with no significant difference ($p > 0.05$), but increased at CW_HR and returned to the same level as upstream at CW_XY.
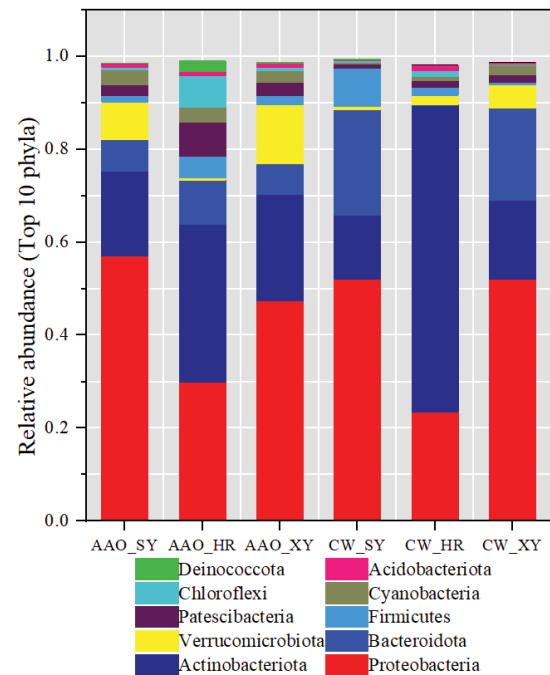
3.3. Differences in abundance at the genus level

At the genus level, the top 50 genera in relative abundance constituted the majority of the overall microbial community structure (80.87% ~ 88.66%), except for the AAO_HR samples, which accounted for only 53.95% of the AAO_HR samples, indicating that AAO effluent discharge inhibited the growth of some genera. The top 50 genera were contained in seven phyla belonging to *Proteobacteria* (20), *Actinobacteriota* (17), *Bacteroidota* (6), *Firmicutes* (3), *Verrucomicrobiota* (2), *Chloroflexi* (1), and *Cyanobacteria* (1). All these phyla and genera are dominant and representative of the overall microbial community structure.

There were large differences in the abundance of the same dominant genera in AAO and CW receiving rivers. The most abundant genera in the AAO_SY included *Sphingorhabdus* (32.19%), *Luteolibacter* (6.94%), *Candidatus_Aquiluna* (3.4%), *unclassified_f_Alcaligenaceae* (2.87%), and *Rhodococcus* (2.81%). The most abundant genera in the AAO_XY included *Sphingorhabdus* (25.49%), *Luteolibacter* (10.95%), *Nocardioides* (6.94%), *Brevundimonas* (6.5%), and *Flavobacterium* (2.9%). The most abundant genera in the CW_SY included *Sphingorhabdus* (30.79%), *Flavobacterium* (19.38%), *Exiguobacterium* (6.53%), *unclassified_f__Alcaligenaceae* (3.67%), and *Brevundimonas* (2.97%). The most abundant genera in the CW_XY included *Sphingorhabdus* (30.76%), *Flavobacterium* (5.8%), *Limnohabitans* (5.73%), *Pseudarcicella* (5.61%), and *Actinokineospora* (5.28%) (Fig. 4). It can be found that the abundance and species of some of the dominant genera in the lower reaches of the two receiving rivers have changed, indicating that wastewater discharges from sewage treatment plants have affected the life activities of the dominant genera in the rivers.
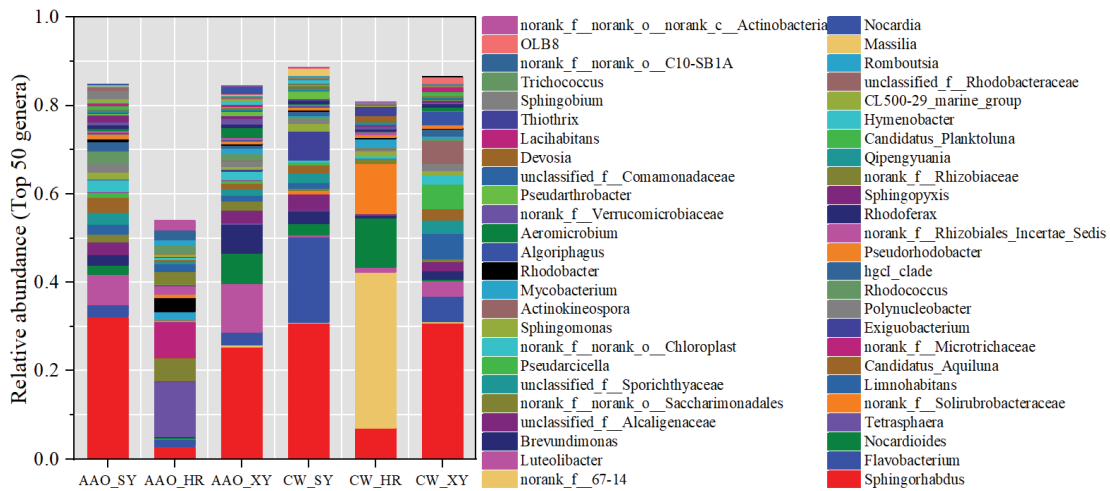
Fig. 4. Stacked histogram of the 50 most abundant dominant genera in relative abundance.

Sphingorhabdus was the most abundant genus in both receiving rivers, and studies have shown that this genus can perform short-range nitrification and denitrification for phosphorus removal [20] and has also been shown to have the potential to degrade hydrocarbons [21]. However, this study showed that changes in COD, TN, TP, and NH_3–N concentrations in the two receiving rivers followed the opposite trend of *Sphingorhabdus* abundance. When pollutant concentrations decreased downstream of the receiving rivers, *Sphingorhabdus* abundance returned to nearly the same level as upstream. *Luteolibacter* is the second-most abundant genus in the AAO receiving river. It has been reported that *Luteolibacter* can be used as a bacterial indicator of good water quality levels in freshwater lakes [22], and similar conclusions were obtained in the present study. The abundance of the genus showed an opposite trend to the change in the concentration of the four pollutants, and life activity was again better restored downstream of the two receiving rivers. Notably, *Luteolibacter* abundance increased by 4.01% in AAO_XY compared to AAO_SY, suggesting that the AAO receiving river has better self-purification ability in terms of pollutant degradation than the CW receiving river. *Tetrasphaera* was the most abundant genus in the AAO WWTP (Fig. S2), so not surprisingly, *Tetrasphaera* abundance increased by 12.44% in the AAO_HR. *Tetrasphaera* is a dominant phosphorus-aggregating organism (PAO) [23] that contributed to the removal of phosphorus pollutants from the AAO receiving river. It is also worth noting that *norank_f__67-14* abundance increased by 35.05% at CW_HR, but this genus was not a dominant genus at the CW WWTP (Fig. S2), with only 0.0095%. A related study showed that the genus was positively correlated with TP concentration [24]. It also showed a positive correlation trend with TP concentration changes in this study, and may also play a role in degrading TP in the CW receiving river, contributing to the reduction of TP concentrations downstream of the CW receiving river.

Fold change confirms the extent to which WWTP influences the structure of river microbial communities [14]. The $\log_2$ fold change analysis method was applied to the change in abundance of the top 50 genera (Fig. S3), comparing the fold change in the difference in abundance of microbial genera downstream and at the confluence with upstream, respectively. There were 33 dominant genera in AAO_HR with decreased abundance (negative $\log_2$ fold change) and 17 dominant genera with increased abundance (positive $\log_2$ fold change), with a mean $\log_2$ fold change of –1.59. This indicates that the total abundance of dominant genera in AAO_HR was suppressed by the effluent discharge, with a 1.59-fold decrease in abundance, consistent with the total decrease in abundance of the AAO_HR samples in Fig. 4. In AAO_XY there was a decrease in abundance of 29 dominant genera, an increase in abundance of 20 dominant genera, and a return to the same level as upstream for only one genus (*Thiothrix*), whose abundance was unchanged ($\log_2$ fold change = 0) with a mean $\log_2$ fold change of 0.23, indicating an increase in the sum of abundance of dominant genera in AAO_XY. At CW_HR, 26 dominant genera decreased in abundance, 22 dominant genera increased in abundance, and only one genus (*Nocardia*) remained unchanged in abundance. Also, *norank_f__norank_o__C10-SB1A* was not present in receiving rivers, and CW effluent discharges did not contain this genus (but AAO effluent did). The mean $\log_2$ fold change of –1.29 indicates that the total abundance of the dominant genus in CW_HR was reduced by a factor of 1.29, which is lower than the reduction in total abundance in AAO_HR. There were 21 dominant genera with reduced abundance and 28 dominant genera with increased abundance in CW_XY, but the mean $\log_2$ fold change was –0.03, indicating that the total abundance of dominant genera in AAO_XY was reduced. The CW effluent discharge supplemented the receiving river with a new dominant genus (*Actinokineospora*, an actinomycete genus), and this genus was absent upstream but significantly increased downstream ($\log_2$ fold change = 11.23) ($p < 0.05$). This result is attributed to the fact that most *Actinokineospora* spp. are aerobic [19] and that higher dissolved oxygen concentrations in the river than in CW promoted the rapid growth of this genus.

The present study remarkably analyzed the degree of dispersion of the $\log_2$ fold change values downstream of the two WWTPs. The results showed that the AAO_XY dominant genus abundance was less discrete (ANOVA of 3.41

and 7.79 for AAO_XY and CW_XY, respectively), indicating that the AAO receiving river is better able to recover from changes in microbial community abundance, consistent with the results obtained from analyzing trends in *Luteolibacter* abundance. This result may be explained by the fact that microorganisms in the aeration environment of AAO are more easily adapted to receiving rivers with higher dissolved oxygen and can rapidly degrade pollutants within a short distance.

3.4. Effects of environmental factors on river microbial communities

Based on db-RDA, this paper analyzed the relationship between changes in mean concentrations of pollutants (COD, TN, TP, and NH$_3$–N) and the horizontal structure of microbial genera in receiving rivers (Fig. 5). The db-RDA analysis explained 58.71% of the samples as a whole and showed that COD had the greatest impact on the samples. The results revealed a large change in sample position for both AAO_HR and CW_HR, also indicating the relative impact of effluent discharge on receiving rivers. The AAO_XY and CW_XY sample positions shifted to the left and right, respectively, but the CW upstream and downstream sample positions were closer together, indicating that CW effluent discharge has less impact on the receiving river, or that river is more resistant to CW effluent discharge. This result is inconsistent with the analysis of greater dispersion in the multiplicity of differences in abundance of dominant genera and may be related to the underrepresentation or number of dominant genera.

The top 50 genera in terms of relative abundance were further analyzed for correlation with nine environmental factors (DO, Temperature, pH, flow rate, Altitude, NH$_3$–N, TN, TP, and COD), as shown in Fig. 6. Temperature, Altitude, NH$_3$–N, TN, TP, and COD were significantly positively correlated ($p < 0.05$) with 4, 7, 4, 1, 2, and 2 dominant genera, respectively, and negatively correlated ($p < 0.05$) with 1, 0, 5, 3, 9, and 7 dominant genera, respectively.
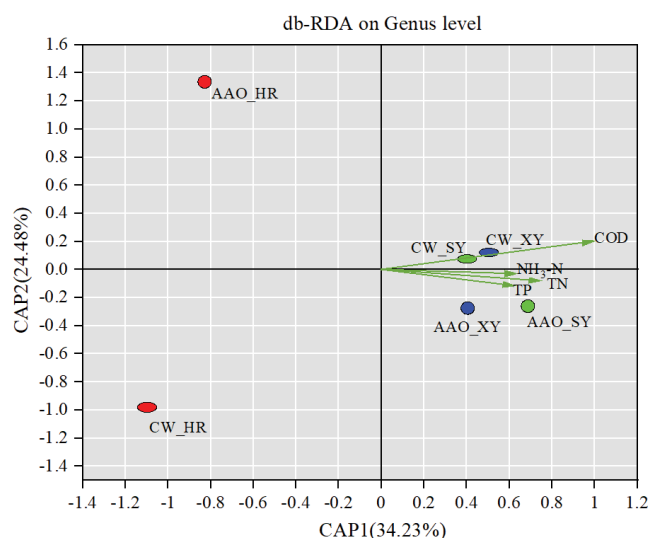
DO was significantly negatively correlated only with *unclassified_f__Comamonadaceae*, and pH and flow rate were significantly positively correlated only with *OLB8* and *Sphingobium*, respectively. Most of the dominant genera that were significantly affected belonged to specific functional genera. *Sphingorhabdus* was the dominant genus with the highest abundance in this study. It has been described as a degrader of polycyclic aromatic hydrocarbons (PAHs) [25,26] and was significantly negatively correlated with COD. *Brevundimonas* have been shown to have a low tolerance to organic pollutants in the aquatic environment and a negative correlation with COD concentrations [27], and this study showed the same trend of influence. *Tetrasphaera* is the dominant phosphorus-aggregating organism (PAO) [23] and showed a significant positive correlation with TP concentrations. *Rhodobacter*, a typical genus of denitrifying bacteria [28], was closely associated with NH$_4^+$–N and NO$_3^-$–N [29] and showed a significant positive correlation with NH$_3$–N in the present study (Fig. 6).

3.5. Effects of sewage discharge on carbon metabolism

According to the changes in water quality indicators in receiving rivers, sewage discharge contains a large amount of nutrients, and the main nutrient increases are COD, TN, NH$_3$–N, and TP. This study shows an increase or decrease in the abundance of some functional microorganisms in the river and an increase or decrease in the abundance of functional modules in the metabolic pathways of carbon, nitrogen, and phosphorus in the river as well.

Carbon metabolism is the most fundamental and important metabolic pathway in the entire life cycle of microorganisms. It consists of three secondary metabolic pathways: carbohydrate metabolism, amino acid metabolism, and energy metabolism. Next, the three secondary metabolisms contain a total of 47 functional modules, and the differential multiplicity of their abundance is shown in Fig. S4.
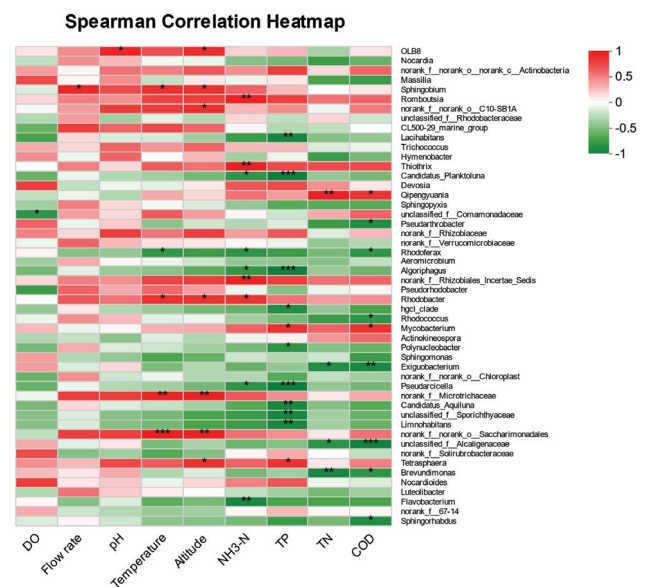

Fig. 5. db-RDA on genus level.

Fig. 6. Spearman correlation heatmap on genus level.

The results show that the abundance of the 47 functional modules showed an increase or decrease at the confluence and downstream compared to upstream. The only difference concerns the different multiplicities of increase or decrease. In addition, most of the functional modules increased in abundance in CW_HR and only four decreased in abundance, while an equal number of increases and decreases in abundance were observed in AAO_HR, indicating that the effects of different sewage treatment processes on river carbon metabolism are variable. Notably, the results of the dispersion analysis of the multiplicity of differences in functional module abundance in AAO_XY (ANOVA = 0.02) were found to be smaller than in CW_XY (ANOVA = 0.12), indicating that the AAO receiving river shows a stronger recoverability to changes in carbon metabolism pathways.

Methane oxidation (M00174), non-phosphorylative Entner–Doudoroff pathway (M00309), and methanogenesis (M00567) all increased significantly in abundance at the confluence of both AAO and CW nepheloid reaches ($\log_2$ fold change > 1.3) ($p < 0.05$). Four functional modules, including Entner–Doudoroff pathway (M00008), Serine biosynthesis (M00020), CAM (Crassulacean acid metabolism, dark) (M00168), semi-phosphorylative Entner–Doudoroff pathway (M00633), showed completely opposite trends in abundance at and downstream of the confluence of the AAO and CW nepheloid reaches. For example, M00633 showed a decrease ($\log_2$ fold change = –0.49) and an increase ($\log_2$ fold change = 0.44) in abundance at the AAO confluence and downstream, and an increase ($\log_2$ fold change = 0.74) and a decrease ($\log_2$ fold change = –2.05) at the CW confluence and downstream. And the only abundance difference fold reduction in CW_XY for this module was more than 2-fold.

3.5.1. Carbohydrate metabolism

The carbohydrate metabolic pathway comprises central carbohydrate metabolism and other carbohydrate metabolism, with a total of 21 functional modules. Central carbohydrate metabolism: glycolysis (Embden-Meyerhof pathway (M00001), core module involving three-carbon compounds (M00002)), pyruvate oxidation (M00307), citrate cycle (TCA cycle (M00009), first carbon oxidation (M00010), second carbon oxidation (M00011)), pentose phosphate pathway ((pentose phosphate cycle (M00004), oxidative phase (M00006), non-oxidative phase (M00007), archaea (M00580)), PRPP biosynthesis (M00005), Entner–Doudoroff pathway (M00008), semi-phosphorylative Entner–Doudoroff pathway (M00308, M00633), non-phosphorylative Entner–Doudoroff pathway (M00309). Other carbohydrate metabolism: glyoxylate cycle (M00012), ethylmalonyl pathway (M00373), methylaspartate cycle (M00740), photorespiration (M00532), malonate semialdehyde pathway (M00013), propanoyl-CoA metabolism (M00741).

As shown in Fig. S4, all 21 functional modules in the carbohydrate metabolic pathway were affected by the effluent discharge, with seven of them (M00006, M00307, M00580, M00633, M00309, M00013, and M00741) in particular being significantly affected ($p < 0.05$). It showed a significant increase or decrease in abundance at the confluence of the two receiving rivers and downstream. In particular, the M00309 and M00013 functional module pathways

were incomplete and lacked expression of some key genes. The trends in gene abundance in the other five functional modules specifically influenced by effluent discharge are shown in Fig. 7.

Key genes in M00633 included *gnaD*, *kdgK*, *gapN*, and *eda* (Fig. 7a). *gnaD* abundance was less affected by effluent discharge and expressed at lower levels in the AAO receiving river, but increased significantly ($p < 0.05$) in CW_HR abundance, indicating a greater impact from effluent discharge, before recovering to expression levels close to those upstream and downstream. *kdgK* abundance was significantly lower ($p < 0.05$) at the confluence of both effluent-contaminated reaches, and both recovered expression levels downstream. *gapN* was not significantly different ($p > 0.05$) across the AAO receiving river, but significantly reduced ($p < 0.05$) at the CW confluence and downstream, and did not recover to better expression levels downstream. *eda* decreased at AAO_HR and recovered to the same expression level downstream as upstream. *eda* increased at CW_HR and decreased at CW_XY.

The M00307 functional module involved the expression of more key genes, denoted as enzymes *E1.2.7.1* and *E1.2.4.1*, respectively (Fig. 7a). *E1.2.7.1* was significantly increased in both AAO_HR and CW_HR ($p < 0.05$) and returned to the same expression level as upstream and downstream. *E1.2.4.1* showed no significant change ($p > 0.05$) in the AAO nadir but increased significantly and was highly expressed in CW_HR.

The changes in gene abundance in the M00006 and M00580 functional modules were reversed, and gene abundance was higher in the M0006 module than in M00580 (Fig. 7b). The abundance of genes involved in the M00006 functional module (G6PD, PGLS, and PGD) increased at the AAO confluence and downstream, but increased at CW_HR and decreased at CW_XY. The abundance of genes involved in the M00580 functional module (*hxlB*, *hxlA*, and *hps-phi*) all decreased at AAO_XY and CW_XY. Among them, *hps-phi*, a common key gene involved in the material transformation of Fructose-6P ↔ arabino-3-Hexulose-6P ↔ Ribulose-5P, was significantly increased in CW_XY ($p < 0.05$). The *rpiAB* abundance showed no significant change ($p > 0.05$) in the AAO nadir and increased significantly ($p < 0.05$) in CW_HR. In particular, *rpiAB* abundance was significantly higher than the other genes in this functional module, most possibly due to the direct influence of the M00006 functional module.

M00741 is an important metabolic pathway in carbon metabolism with high functional module abundance and gene abundance (Fig. 7c). *bccA*, *PCCA*, *PCCB*, *MCEE*, *E5.4.99.2AB*, and *MUT* are key genes in the M00741 pathway. They are inconsistently affected by effluent discharge in the AAO and CW natal reaches, but have in common good recoverability downstream. *bccA*, *MCEE*, and *E5.4.99.2AB* abundance all increase at AAO_HR and CW_HR, while PCCA and *MUT* decrease at the confluence. *PCCB* differs from them, decreasing at AAO_HR and increasing at CW_HR.

3.5.2. Methane metabolism

Methane metabolism contains a total of nine functional modules: methanogenesis (M00567, M00357, M00356,
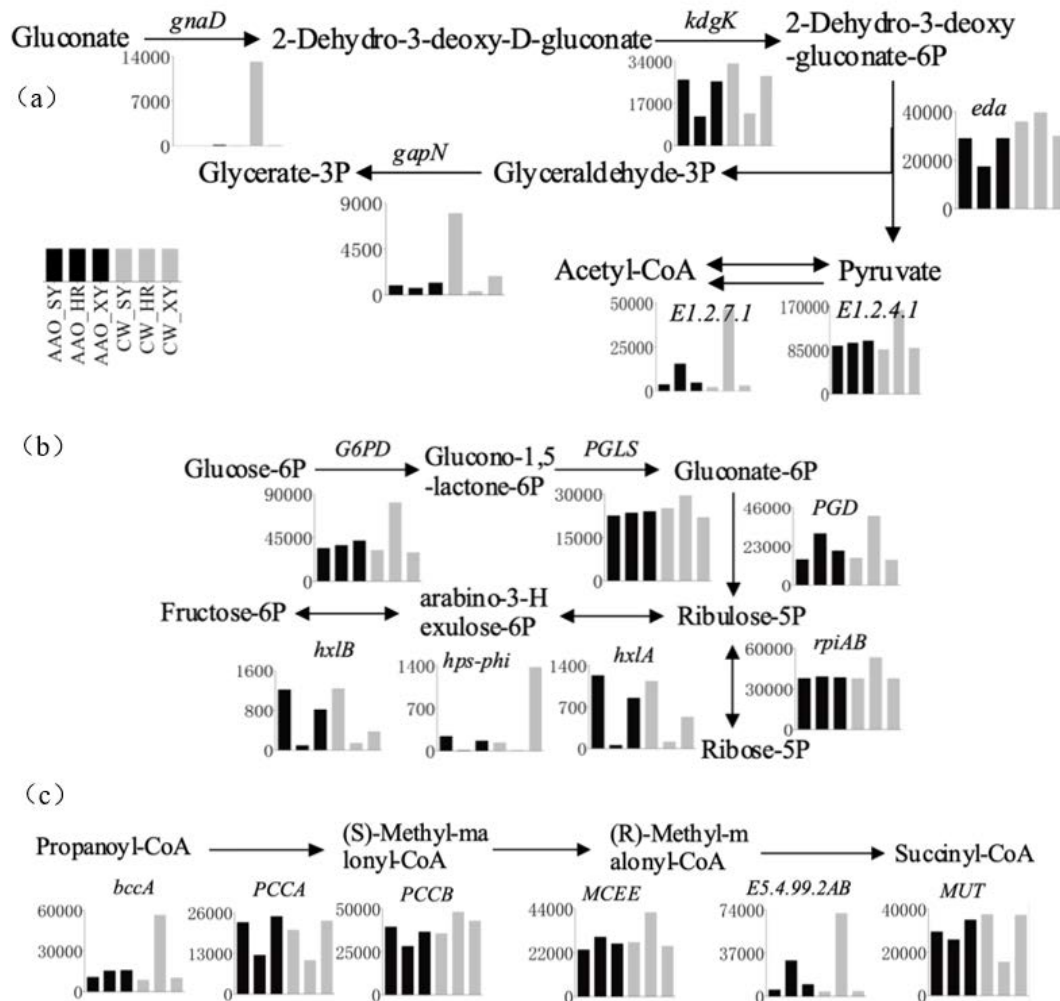
Fig. 7. Selected functional module pathways in carbohydrate metabolism (a) M00633, M00307, (b) M00006, M00580 and (c) M00741. (Bar graphs with sample names from left to right on the horizontal axis are AAO_SY, AAO_HR, AAO_XY, CW_SY, CW_HR, CW_XY and the vertical axis indicates the absolute abundance of key genes).

M00563), methane oxidation (methanotroph) (M00174), formaldehyde assimilation (serine pathway (M00346), ribulose monophosphate pathway (M00346), xylulose monophosphate pathway (M00344)), and acetyl-CoA pathway (M00422). As shown in Fig. S4, the abundance of all functional modules of carbon metabolism was effected by effluent discharge as a result of effluent discharge upon gene expression. In Fig. S4, it is shown that of all functional modules of carbon metabolism, six functional modules of methane metabolism (M00174, M00567, M00422, M00563, M00356, and M00357) were all significantly affected by relatively large fold differences in abundance at and downstream of the confluence of the two effluent-bearing river segments, AAO and CW ($p < 0.05$). Therefore, specific trends in the abundance of the major participating genes or enzymes in the six functional module pathways are further demonstrated, as shown in Fig. 8.

Methanogenesis pathway involves four functional modules, and their expression levels of the genes involved differ considerably among them. The variation in the abundance of genes in the two receiving rivers, AAO and CW, was highly variable. However, most gene abundances increased at the confluence, consistent with Fig. S4 showing trends in functional module abundance, indicating that changes in functional module abundance are a further reflection of changes in gene or enzyme abundance.

mdh12, ftr, fwdABC, mch, and *cooSF* abundance increased significantly at AAO_HR ($p < 0.05$) but less at CW_HR. *PmoC-amoC, hdrB2, dmd-tmd, mer, ACSS1_2*, and *cdhE* increased less at AAO_HR but significantly at CW_HR. *mcrA, mtaB, mtbB, mtmB, mtd*, and *mtrH* increased significantly ($p < 0.05$) at AAO_HR and remained unchanged or even decreased in abundance at CW_HR. However, they showed a small overall gene abundance and appeared to be insignificant for the overall expression of metabolic pathways. *pta* abundance decreased at the confluence of both receiving rivers, but increased and decreased at AAO_XY and CW_XY, respectively.

3.6. Effects of effluent discharge on nitrogen metabolism pathways

Nitrogen metabolism is the main pathway for the removal of pollutants such as total nitrogen and ammonia
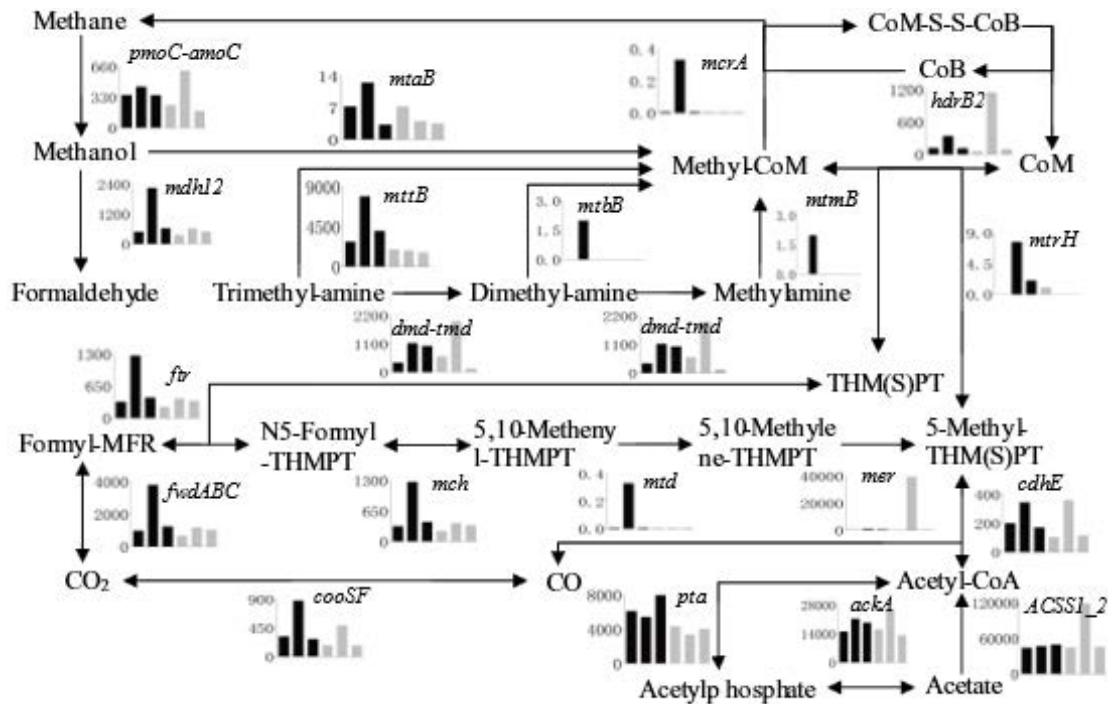
Fig. 8. Methane metabolism pathway. (Bar graphs with sample names from left to right for AAO_SY, AAO_HR, AAO_XY, CW_SY, CW_HR, CW_XY on the horizontal axis and absolute abundance of key genes on the vertical axis).

nitrogen. Nitrogen metabolism consists of six functional modules: nitrogen fixation (M00175), assimilatory nitrate reduction (M00531), dissimilatory nitrate reduction (M00530), nitrification (M00528), denitrification (M00529), and complete nitrification (M00804).

According to the fold change in differential abundance shown (Fig. S5), both WWTPs had a significant effect ($p < 0.05$) on the six functional modules of nitrogen metabolism at the confluence and downstream in receiving rivers compared to upstream. The dispersion in the multiplicity of differences in abundance of functional modules was smaller in CW_XY (ANOVA = 0.075) than in AAO_XY (ANOVA = 0.107), indicating that the CW receiving river showed a stronger recoverability to changes in nitrogen metabolism pathways. In AAO_HR, three functional modules, M00175, M00529, and M00804, showed positive and greater than 1-fold changes in abundance difference multiples. Three functional modules, M00531, M00530, and M00528, had smaller increases in abundance difference multiples. In CW_HR, all six functional modules have a more than 1-fold increase in abundance difference multiples. It is worth noting that M00804 has the largest increase in multiples in the two receiving river sections, 2.62 and 3.86 times, respectively, indicating that it is most influenced by sewage discharge, followed by M00529.

Many genes and enzymes are involved in the nitrogen metabolism pathway, as illustrated in Fig. 9, which shows some key genes. *narGHI*, *nirK*, *norB*, and *nosZ* are the key genes in the Denitrification functional module of nitrogen metabolism in this study. The abundance of *narGHI* was significantly increased at both AAO_HR and CW_HR, and the abundance of *nirK*, *norB*, and *nosZ* was significantly

increased at AAO_HR and not significantly different from downstream at the confluence ($p > 0.05$), but decreased at CW_HR. The differences in *norB* and *nosZ* abundance were greater between CW_XY and CW_SY and failed to return to expression levels similar to those upstream, indicating that effluent discharge had a greater impact on gene expression in the denitrification functional module in the CW catchment. This further suggests that the AAO nullah section has better recovery of denitrification functional module gene expression. In addition, the special natural environment of the plateau has been reported to affect the rate of denitrification of nitrogen metabolism in rivers, which is significantly lower than other rivers in the plains [30]. *nifDKH*, a key gene in the nitrogen fixation functional module, showed similar trends in both the AAO and CW receiving rivers, both significantly increasing at the confluence. *hao* and *pmoC-amoC* were key genes in the nitrification functional module, and both genes showed similar trends, but hao abundance was lower, indicating that it was not the main denitrification process in receiving rivers. It has been shown that nitrification dominates nitrogen cycling below WWTP outfalls [12]. This result differs from the present study mainly due to the specific plateau environment.

The key genes involved in M00531 contained *nasC* and *nirA*. *nirA* did not change significantly ($p > 0.05$) in the AAO receiving river. However, there was a highly significant increase in CW_HR ($p < 0.01$), and expression levels were restored downstream. *nasC* increased at AAO_HR and AAO_XY, and decreased and increased at CW_HR and CW_XY, respectively. M00530 and M00531 metabolic pathways were similar, but involved different key genes, which contained *narGHI* and *nirBD*. *narGHI* is also involved
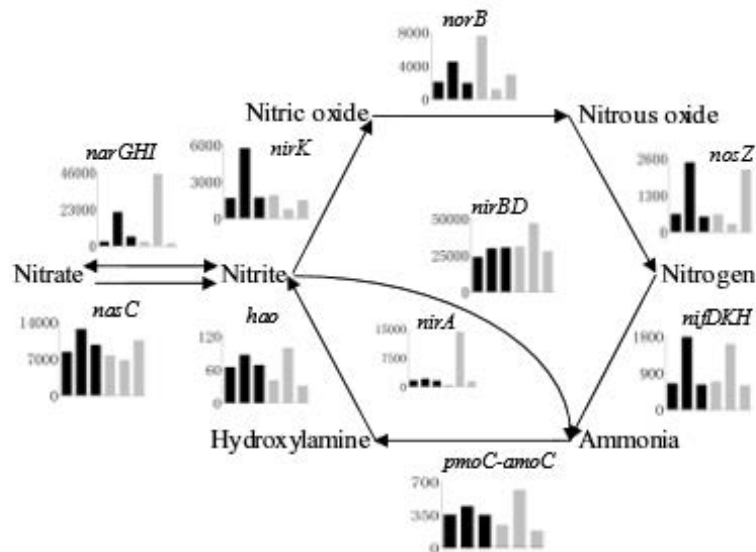
Fig. 9. Nitrogen metabolic pathways. (Bar graphs with sample names from left to right for AAO_SY, AAO_HR, AAO_XY, CW_SY, CW_HR, CW_XY on the horizontal axis and absolute abundance of key genes on the vertical axis).

in the response of the denitrification functional module, consistent with the previous analysis. *nirBD* was significantly increased in CW_HR, with no significant difference ($p > 0.05$) across the entire nitrogen-holding rivers in AAO, and its abundance was higher in the entire nitrogen metabolism pathway, indicating that M00530 is the main denitrification process in receiving rivers. The pathway in complete nitrification was partially consistent with the nitrification pathway with the addition of a material transformation pathway (nitrite → nitrate), and the key genes involved were *narGH*. Notably, the trends of TN and NH_3–N concentrations in the two receiving rivers were consistent with the trends of gene abundances involved in the complete nitrification metabolic pathway. And the gene abundance increased more at CW_HR compared to upstream, probably due to the greater TN and NH_3–N concentrations provided by the CW WWTP.

3.7. Effects of effluent discharge on phosphorus metabolism

Oxidative phosphorylation contains 21 functional modules, but only 17 functional modules were present in this study: NADH dehydrogenase (ubiquinone) Fe–S protein/flavoprotein complex, mitochondria (M00143), NADH: quinone oxidoreductase, prokaryotes (M00144), NAD(P)H: quinone oxidoreductase, chloroplasts and cyanobacteria (M00145), NADH dehydrogenase (ubiquinone) 1 Alpha subcomplex (M00146), succinate dehydrogenase, prokaryotes (M00149), fumarate reductase, prokaryotes (M00150), cytochrome bc1 complex respiratory unit (M00151), cytochrome bc1 complex (M00152), cytochrome c oxidase (M00154), cytochrome c oxidase, prokaryotes (M00155), cytochrome bd ubiquinol oxidase (M00153), cytochrome o ubiquinol oxidase (M00417), cytochrome aa3-600 menaquinol oxidase (M00416), cytochrome c oxidase, cbb3-type (M00156), F-type ATPase, prokaryotes and chloroplasts (M00157), F-type ATPase, eukaryotes (M00158), V/A-type ATPase, prokaryotes

(M00159). Four missing functional modules: succinate dehydrogenase (ubiquinone) (M00148), V-type ATPase, eukaryotes (M00160), NADH: ubiquinone oxidoreductase, mitochondria (M00142), NADH dehydrogenase (ubiquinone) 1 beta subcomplex (M00147).

The 17 functional modules were differentially affected in each of the two receiving rivers, AAO and CW. The dispersion in the fold difference in abundance of functional modules was smaller in AAO_XY (ANOVA = 0.18) than in CW_XY (ANOVA = 1.005), indicating that the AAO receiving river showed greater resilience to changes in oxidative phosphorylation metabolic pathways. The abundance of functional modules M00145, M00151, M00152, M00153, and M00416 showed exactly opposite trends in the confluence and downstream of the two receiving river sections (Fig. S6), indicating that different sewage treatment processes had opposite effects on these functional modules mentioned above. Furthermore, the abundance of modules M00146 and M00159 increased significantly at AAO_HR (log$_2$ fold change of 2.49 and 2.72, respectively) ($p < 0.05$). In particular, M00158 decreased at AAO_HR (log$_2$ fold change = –2.6) but increased more at CW_HR (log$_2$ fold change = 7.44). M00413, M00145, and M00416 increased or decreased significantly in both CW_HR and CW_XY but failed to revert to the same or similar abundances as upstream in CW_XY, indicating that the CW neritic reaches showed no better resistance to changes in the abundance of functional modules M00413, M00145, and M00416.

The genes partially involved in phosphorus metabolism are illustrated in Fig. 10. *ATPF0ABC/ATPF1ABDEG*, *ATPVABCDEFIK*, and *ATPeF0O* are the key genes involved in the interconversion of ATP and ADP. *ATPF0ABC/ATPF1ABDEG* showed a flat trend in the two receiving river segments AAO and CW and was not significantly influenced by effluent discharge ($p > 0.05$). *ATPVABCDEFIK* increased significantly at AAO_HR and to a lesser extent at CW_HR. *ATPeF0O* was not significantly different ($p > 0.05$) in the AAO
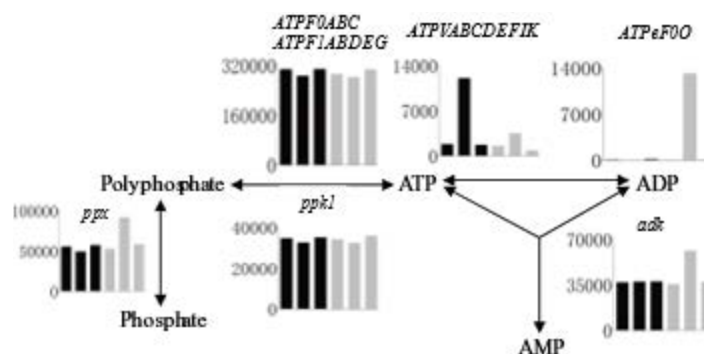
Fig. 10. Phosphorus metabolic pathways. (Bar graphs with sample names from left to right on the horizontal axis are AAO_SY, AAO_HR, AAO_XY, CW_SY, CW_HR, CW_XY and the vertical axis indicates the absolute abundance of key genes).

effluent-bearing reaches, increased significantly in CW_HR, and resumed expression levels in all downstream reaches. *ppk1*, a key gene in the synthesis of polyphosphate from ATP substrates, was not significantly different in either receiving river. *ppx*, a key gene in the hydrolysis of polyphosphate to phosphate, was not significantly different in the AAO receiving river, but significantly increased in CW_HR. It was notable that *adk* was almost unaffected by effluent discharge in the AAO receiving river, but significantly increased in CW_HR, similar to the trend of *ppx* gene expression.

4. Conclusions

This study compares the effects of two municipal sewage treatment processes on receiving rivers in a plateau habitat. In terms of water quality indicators, the AAO receiving river has a better self-purification capacity for the pollutants NH$_3$–N, TN, and COD. In particular, the CW receiving river has a better self-purification capacity for NH$_3$–N and TP. Both effluent discharges increased microbial diversity downstream of the two receiving rivers. However, changes in microbial diversity at the confluence are inconsistent, with AAO and CW effluent discharges increasing and suppressing microbial diversity at the confluence, respectively. In addition, the overall microbial diversity of rivers in the plateau environment is lower than that in the plains, indicating that the specific environment of the plateau suppresses microbial diversity. *Proteobacteria* (47.4% ~ 57.04%) and *Sphingorhabdus* (25% ~ 32.19%) were both the most abundant phylum and genus in the upper and lower reaches of the two receiving rivers. *Luteolibacter* served as a bacterial indicator of good water quality levels in freshwater lakes. *Luteolibacter* abundance increased by 4.01% in AAO_XY, indicating that the AAO receiving river has a better self-purification capacity for pollutant degradation than the CW receiving river. In addition, analysis of downstream trends in the abundance of dominant genera also confirmed that the AAO receiving river is better able to recover from changes in microbial community abundance. The degree of influence of AAO and CW WWTP on the microbial community structure of the river was confirmed by the difference in multiplicity, showing significant effects on both dominant phyla and dominant genera. Based on trends in the abundance of dominant genera downstream, the AAO receiving river shows a better ability to recover from changes in microbial community abundance. Effluent discharge also shows significant effects on riverine carbon, nitrogen, and phosphorus metabolic pathways. AAO and CW effluent discharges show differences in the metabolic pathways of the same functional module of the river and even have completely opposite effects on some functional modules. A dispersion analysis of the functional module difference multipliers revealed that the AAO receiving river shows better recoverability in carbon and phosphorus metabolic pathways, and the CW shows better recoverability in nitrogen metabolic pathways.

Author contribution

All the authors contributed to the study's conception and design. Material preparation, data collection, and analysis were performed by Jun Wang, Jiaao Ji, Xianpai Peng, Yongchen Zong, Chunhui Fu, Dongyan Zhang. The first draft of the manuscript was written by Jun Wang, and all the authors commented on the previous versions of the manuscript. All the authors read and approved the final manuscript.

Data availability

Due to the confidentiality of the experimental data and the experimental research being in the basic mechanism research stage, the experimental data will not be disclosed for the time being. The data set generated and/or analyzed during the current research period cannot be publicly obtained but can be obtained from the corresponding author, according to reasonable requirements obtained there. The data in this article can be used after obtaining the consent of all the authors. The email address for obtaining data: wj_3nlzzx@163.com.

Declarations

Ethics approval and consent to participate

Not applicable.

Consent for publication

Not applicable.

Competing interests

The authors declare no competing interests.

References

[1] J. Wang, Y. Zong, C. Fu, M. Guo, J. You, D. Zhang, Study on community structure and nitrogen metabolism mechanism in A²O process under different hydraulic retention time conditions at high altitude region, Global NEST J., 25 (2023) 169–179.

[2] T. García-Armisen, Ö. İnceoğlu, N.K. Ouattara, A. Anzil, M.A. Verbanck, N. Brion, P. Servais, Seasonal variations and resilience of bacterial communities in a sewage polluted urban river, PLoS One, 9 (2014) e92579, doi: 10.1371/journal.pone.0092579

[3] Y.C. Zong, Y.H. Zhang, G.H. Lu, X.Y. Chen, Study on process characteristics of high altitude A²/O process based on principal component analysis, Technol. Water Treat., 44 (2018) 116–119 (in Chinese).

[4] Y. Zong, Y. Li, K. Hao, G. Lu, D. Huang, Influence of transient change of water temperature on pilot-scale anaerobic-anoxic-oxic process under plateau environmental factors, Appl. Ecol. Environ. Res., 17 (2019) 12191–12202.

[5] D. Figueroa-Nieves, W.H. McDowell, J.D. Potter, G. Martínez, J.R. Ortiz-Zayas, Effects of sewage effluents on water quality in tropical streams, J. Environ. Qual., 43 (2014) 2053–2063.

[6] I. Aristi, D. von Schiller, M. Arroita, D. Barceló, L. Ponsatí, M.J. García-Galán, V. Acuña, Mixed effects of effluents from a wastewater treatment plant on river ecosystem metabolism: subsidy or stress?, Freshwater Biol., 60 (2015) 1398–1410.

[7] B.T. Chu, M.L. Petrovich, A. Chaudhary, D. Wright, B. Murphy, G. Wells, R. Poretsky, Metagenomics reveals the impact of wastewater treatment plants on the dispersal of microorganisms and genes in aquatic sediments, Appl. Environ. Microbiol., 84 (2018) e02168-17, doi: 10.1128/AEM.02168-17

[8] B.G. Rahm, N.B. Hill, S.B. Shaw, S.J. Riha, Nitrate dynamics in two streams impacted by wastewater treatment plant discharge: point sources or sinks?, JAWRA J. Am. Water Res. Assoc., 52 (2016) 592–604.

[9] S.N. Merbt, J.C. Auguet, A. Blesa, E. Martí, E.O. Casamayor, Wastewater treatment plant effluents change abundance and composition of ammonia-oxidizing microorganisms in Mediterranean urban stream biofilms, Microbiol. Ecol., 69 (2015) 66–74.

[10] D.D. Lofton, A.E. Hershey, S.C. Whalen, Evaluation of denitrification in an urban stream receiving wastewater effluent, Biogeochemistry, 86 (2007) 77–90.

[11] R.Z. Li, X. Yu, N. Tang, Sediment denitrification rate and its response to exogenous carbon in the stream reach receiving urban sewage treatment plant effluent, Acta Sci. Circumstantiae, 40 (2020) 2539–2547 (in Chinese).

[12] P. Sonthiphand, E. Cejudo, S.L. Schiff, J.D. Neufeld, Wastewater effluent impacts ammonia-oxidizing prokaryotes of the Grand River, Canada, Appl. Environ. Microbiol., 79 (2013) 7454–7465.

[13] R. Guan, H. Yuan, A.C. Wachemo, Effect of narrow feeding regimes on anaerobic digestion performance and microbial community structure of rice straw in continuously stirred tank reactors, Energy Fuels, 32 (2018) 11587–11594.

[14] J.R. Price, S.H. Ledford, M.O. Ryan, L. Toran, C.M. Sales, Wastewater treatment plant effluent introduces recoverable shifts in microbial community composition in receiving streams, Sci. Total Environ., 613 (2018) 1104–1116.

[15] B. Drury, E. Rosi-Marshall, J.J. Kelly, Wastewater treatment effluent reduces the abundance and diversity of benthic bacterial communities in urban and suburban rivers, Appl. Environ. Microbiol., 79 (2013) 1897–1905.

[16] E. Marti, J.L. Balcázar, Use of pyrosequencing to explore the benthic bacterial community structure in a river impacted by wastewater treatment plant discharges, Res. Microbiol., 165 (2014) 468–471.

[17] Y. Zong, K. Hao, G. Lu, Y. Li, D. Huang, Characteristics of the colony structure of A²O processes under different ultraviolet conditions in plateau areas, Environ. Sci. Pollut. Res., 29 (2022) 67941–67952.

[18] X. Chen, K. Hao, Y. Zong, M. Guo, J. You, Q. He, D. Zhang, Effects of ultraviolet radiation on microorganism and nitrogen metabolism in sewage under plateau background, Environ. Sci. Pollut. Res., (2023) 1–18, doi: 10.1007/s11356-023-25965-y.

[19] X.M. Li, The Selective Isolation and Diversity of Actinomycetes of Jiangxi Acidic Soil Samples, Jiangxi Agricultural University, China, 2011. Available at: https://kns.cnki.net/KCMS/detail/detail.aspx?dbname=CMFD2012&filename=1011176031.nh

[20] W. Xiong, S. Wang, N. Zhou, Y. Chen, H. Su, Granulation enhancement and microbial community shift of tylosin-tolerant aerobic granular sludge on the treatment of tylosin wastewater, Bioresour. Technol., 318 (2020) 124041, doi: 10.1016/j.biortech.2020.124041.

[21] A. Avona, M. Capodici, D. Di Trapani, M.G. Giustra, P.G. Lucchina, L. Lumia, G. Viviani, Hydrocarbons removal from real marine sediments: analysis of degradation pathways and microbial community development during bioslurry treatment, Sci. Total Environ., 838 (2022) 156458, doi: 10.1016/j.scitotenv.2022.156458.

[22] D. Guo, J. Liang, W. Chen, J. Wang, B. Ji, S. Luo, Bacterial community analysis of two neighboring freshwater lakes originating from one lake, Pol. J. Environ. Stud., 30 (2021) 111–117.

[23] Y. Tian, H. Chen, L. Chen, X. Deng, Z. Hu, C. Wang, S. Wuertz, Glycine adversely affects enhanced biological phosphorus removal, Water Res., 209 (2022) 117894, doi: 10.1016/j.watres.2021.117894

[24] Z. Nie, Z. Zheng, H. Zhu, Y. Sun, J. Gao, J. Gao, G. Xu, Effects of submerged macrophytes (*Elodea nuttallii*) on water quality and microbial communities of largemouth bass (*Micropterus salmoides*) ponds, Front. Microbiol., 13 (2023) 1050699, doi: 10.3389/fmicb.2022.1050699.

[25] S.G. Silva, A. Lago-Lestón, R. Costa, T. Keller-Costa, Draft genome sequence of *Sphingorhabdus* sp. strain *EL138*, a metabolically versatile Alphaproteobacterium isolated from the gorgonian coral *Eunicella labiata*, Genome Announc., 6 (2018) e00142–18, doi: 10.1128/genomeA.00142-18

[26] Y.F. Wei, L. Wang, Z.Y. Xia, M. Gou, Z.Y. Sun, W.F. Lv, Y.Q. Tang, Microbial communities in crude oil phase and filter-graded aqueous phase from a Daqing oilfield after polymer flooding, J. Appl. Microbiol., 133 (202) 842–856.

[27] X.B. Lü, Y.C. Wu, L.Q. Chen, Characteristics of the bacterioplankton community and their relationships with water quality in Chishui River Basin, Acta Sci. Circumstantiae, 41 (2021) 4596–4605 (in Chinese).

[28] N. Benyoucef, A. Pauss, N. Abdi, C.O. Sarde, H. Grib, N. Mameri, Enhancement of the denitrification performance of an activated sludge using an electromagnetic field in batch mode, Chemosphere, 262 (2021) 127698, doi: 10.1016/j.chemosphere.2020.127698.

[29] X. Zhu, C. Shen, J. Huang, L. Wang, Q. Pang, F. Peng, B. Xu, The effect of sulfamethoxazole on nitrogen removal and electricity generation in a tidal flow constructed wetland coupled with a microbial fuel cell system: microbial response, Chem. Eng. J., 431 (2022) 134070, doi: 10.1016/j.cej.2021.134070.

[30] X. Ling, G. Lu, C. Xue, Environmental and anthropogenic factors affect bacterial community and nitrogen removal in the Yarlung Zangbo River, Environ. Sci. Pollut. Res., 29 (2022) 84590–84599.
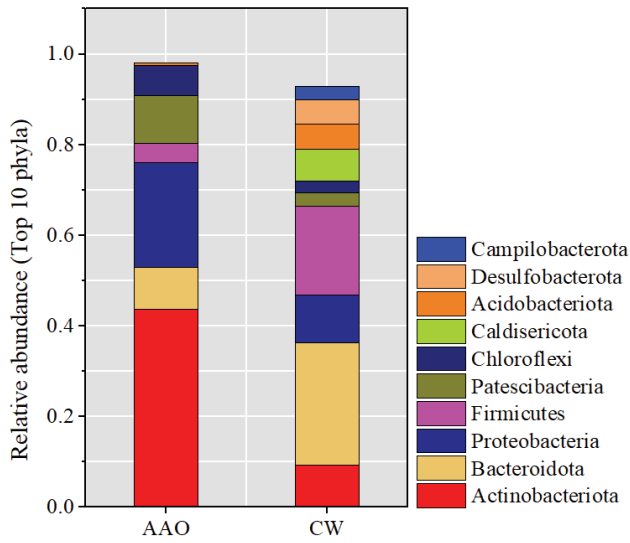
Supporting information

Fig. S1. Stacked histograms of the 10 dominant phyla with the highest relative abundance in AAO and CW WWTPs.
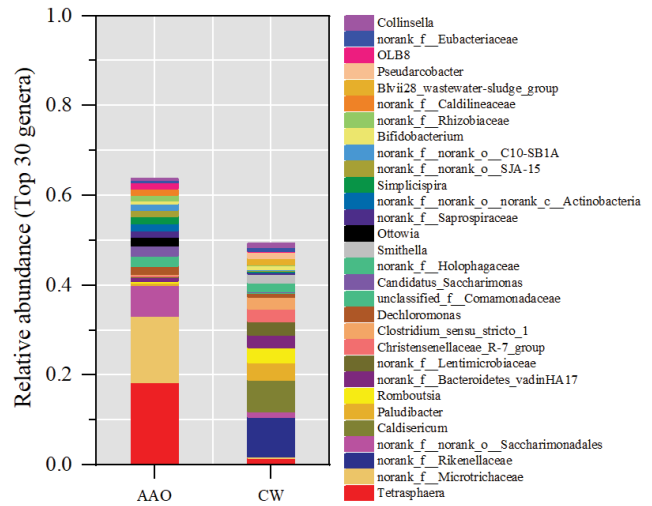

Fig. S2. Stacked histogram of the 30 most abundant dominant genera in relative abundance in AAO and CW WWTPs.
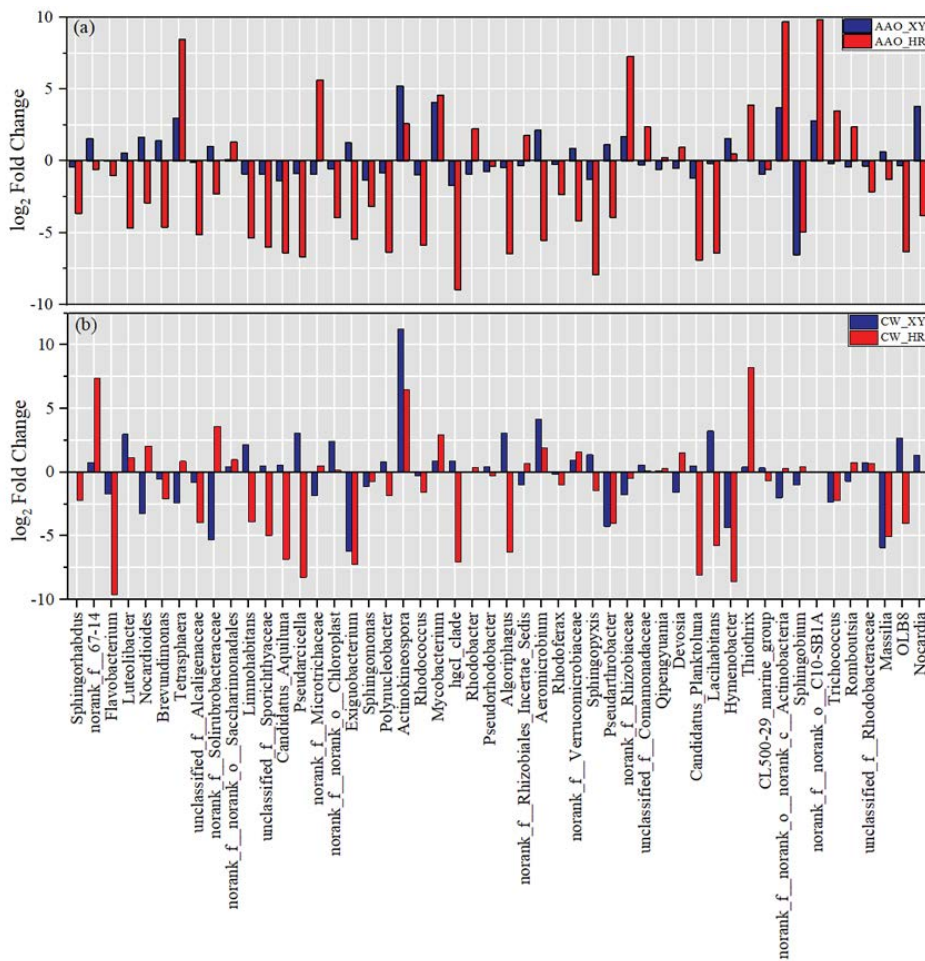

Fig. S3. Log$_2$ fold change for the 50 most abundant dominant genera in relative abundance. (Positive values indicate an increase in folds compared to upstream, negative values indicate a decrease in folds).
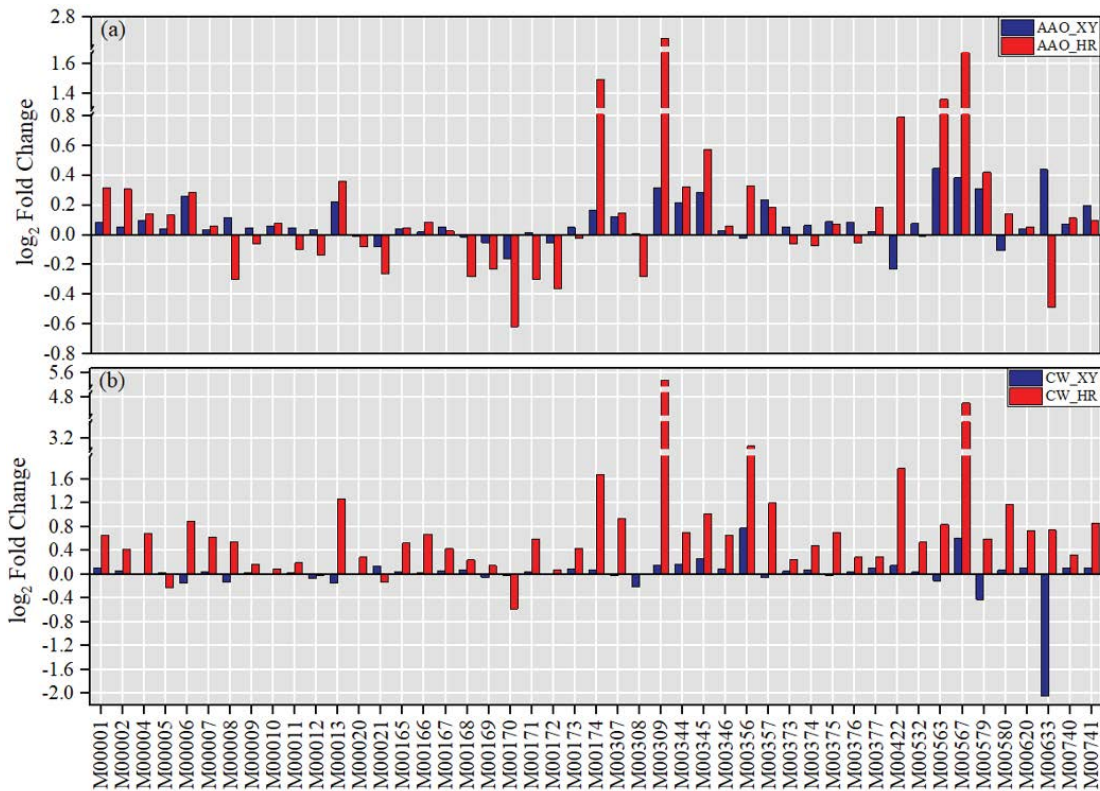
Fig. S4. Log$_2$ fold change for the abundance of 47 functional modules in carbon metabolism. (Positive values indicate an increase in folds compared to upstream, negative values indicate a decrease in folds).
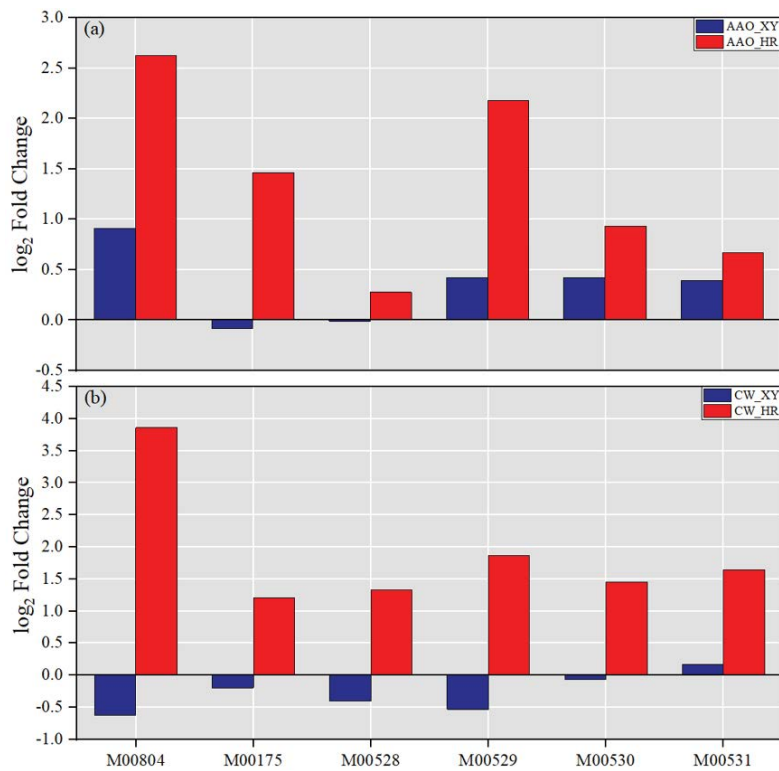

Fig. S5. Log$_2$ fold change in the abundance of 6 functional modules in nitrogen metabolism. (Positive values indicate an increase in folds compared to upstream, negative values indicate a decrease in folds).
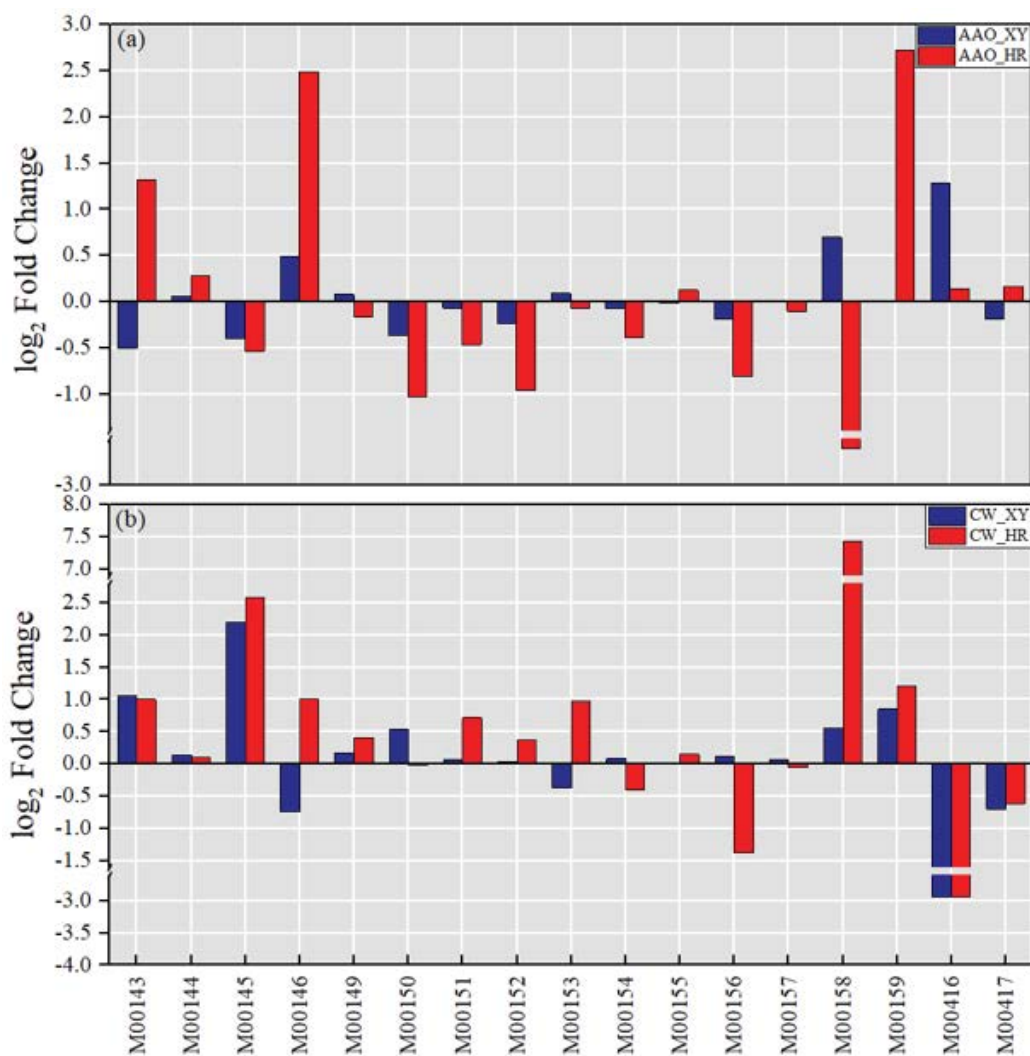
Fig. S6. Log$_2$ fold change in the abundance of 17 functional modules in phosphorus metabolism. (Compared to upstream, positive values indicate an increase in folds, negative values indicate a decrease in folds).

Table S1
Alpha diversity metrics

Sample/estimators	Chao	Shannon	Shannoneven	Coverage
AAO_SY	2,144.28	4.185245	0.574354	0.984352
AAO_HR	1,729.734	5.000443	0.703067	0.989461
AAO_XY	2,209.013	4.360152	0.597077	0.984539
CW_SY	1,784.127	3.640763	0.516858	0.986305
CW_HR	1,809.041	3.472858	0.483732	0.986813
CW_XY	2,006.031	3.894429	0.548255	0.985101